A novel wide-dynamic-range logarithmic-response bipolar junction photogate transistor for CMOS imagers

Xiangliang Jin (金湘亮), Jie Chen (陈 杰), and Yulin Qiu (仇玉林)

Microelectronics R&D Center, Chinese Academy of Sciences, Beijing 100029

Received March 17, 2003

In this paper, a new photodetector, bipolar junction photogate transistor (BJPG), is proposed for CMOS imagers. Due to an injection p^+n junction introduced, the photo-charges drift through the p^+n junction by the applied electronic field, and on the other hand, the p^+n junction injects the carriers into the channel to carry the photo-charges. Therefore this device can increase the readout rate of the pixel signal charges and the photoelectron transferring efficiency. Using this new device, a new type of logarithmic pixel circuit is obtained with a wide dynamic range which makes photo-detector more suitable for imaging the naturally illuminated scenes. The simulations show that the photo current density of BJPG increases logarithmically with the incident light power due to the introduced injection p^+n junction. The noise characteristics of BJPG are analyzed in detail and a new gate-induced noise is proposed. Based on the established numerical analytical model of noise, the power spectrum density curves are simulated.

OCIS codes: 230.0230, 250.0250.

The photodetector and electronic circuits can be integrated into a chip due to the intrinsic photoelectric effect of the standard CMOS process, which results in low cost and low power. Therefore, in recent years, more and more CMOS imaging sensors have been developed[1]. The dynamic range is an important parameter to describe the performance of CMOS imagers[2]. If the CMOS sensor's dynamic range is lower than the scene dynamic range, parts of the image will be clipped in the dark or bright regions. Typically, the dynamic range of CMOS imaging sensor is about 70 dB, which cannot satisfy the application requirements[3]. To increase the dynamic range of CMOS imagers, several approaches have been proposed. One of them is the design of CMOS imaging sensors with logarithmic response[4]. In logarithmic-response CMOS imagers, the I-V characteristics present the logarithmical relation due to a fed resistor that is implemented by a MOS transistor operating in the weak inversion region. The result is that the pixel output signal voltage is logarithmically related with the incident light power. However, the previous techniques depend on the specific circuit design technique and may bring about long integration time, image lag or larger pixel size[5,6].

In this paper, a new photodetector, bipolar junction photogate transistor (BJPG), is proposed for CMOS imaging sensors. Using this new device, a new type of logarithmic pixel circuit is presented with a wide dynamic range. The photo-detector noise characteristic is one of the key factors restricting the performance of the CMOS imagers[7,8]. The noise magnitude decides the resolution and the dynamic range of the readout circuit.

Figure 1(a) illustrates the cross-section view of BJPG on p-Si substrate. Comparing the new device with the traditional photogate transistor, there are two basic differences. The first one is that, an injection p^+n junction is introduced and fabricated in the n-well, which isolates the collected charges under the gate oxide from the floating diffusion p^+ region. The second is the operation principle difference. When the light signal transits the clarity MOS gate to reach the exhaust region (the silicon surface), the electron-hole pairs will be produced. Under the effect of the gate voltage, the majority carriers (hole) will be excluded into the silicon substrate and the minority carriers (electron) are collected in the MOS capacitance potential trap to form the signal charges. In the BJPG, the p^+n junction injects the carriers (hole) into the channel to carry the photo-charges. The photocurrent is composed of both the drift current and the compound current, and therefore the bipolar junction photogate may increase the photo-charges readout rate and improve the operating speed of CMOS imaging sensor. In fact, the behavior of the BJPG is equivalent to the function of both a traditional photogate and a positive bias diode in series, as shown in Fig. 1(b). The fictitious port 'P' is introduced to model the incident light power. The fictitious M is the "drain" of the traditional photogate. The diode completes the logarithmical current-voltage characteristic in the logarithmical pixel with a MOS transistor operating in the weak inversion region.

Figure 2(a) is the traditional logarithmic pixel circuit. Assuming the load MOSFET operating in the subthreshold region, the channel current in load transistor is $I_{\rm ds} = I_0 \exp(qV_{\rm gs}/nkT)$. Therefore the photo-current $I_{\rm ph}$ and the output voltage V_{p1} arise from the subthreshold characteristics of the load transistor[5],

$$V_{p1} = V_{\rm bias} - \frac{nkT\ln(I_p/I_0)}{q}. \tag{1}$$

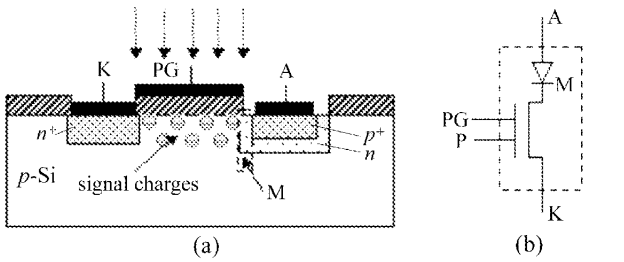

Fig. 1. (a) Cross-section view of BJPG on p-Si substrate; (b) equivalent circuit.

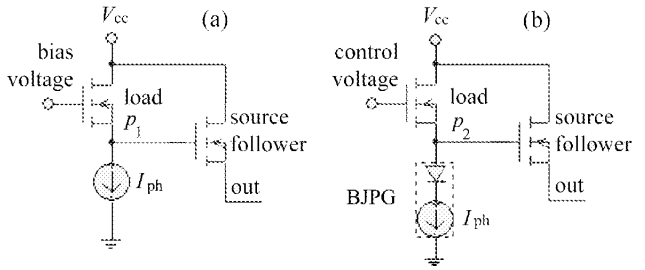

Fig. 2. Traditional logarithmic pixel circuit; (b) new logarithmic pixel circuit.

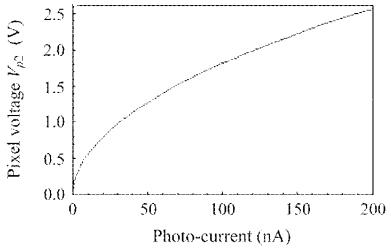

Fig. 3. Simulation result for the new logarithmic pixel circuit.

In the new logarithmic pixel circuit, the load device operates at the switch state under the control voltage and the diode completes the logarithmical current-voltage characteristic. Supposing that the photocurrent can completely convert into the p^+n junction current and the voltage dropping along the n-well region can be ignored, the relationship between the photo-current $I_{\rm ph}$ and the output voltage V_{p2} will be

$$V_{p2} = \frac{kT}{q}\ln(\frac{I_{\rm ph}}{I_0} + 1) + V_{\rm M}. \tag{2}$$

To describe the physical process of the photo-charges in a quantitative way, the MOS potential trap is firstly considered. When the voltage $V_{\rm PG}$ adds up to or larger than the threshold voltage $V_{\rm T}$, the MOS potential trap will attract a lot of the photoelectrons (with the charge of $Q_{\rm S}$) generated by the incident light. Assuming that there are no majority carriers in the depletion region. Therefore, the expression of the surface potential[9], which is an important physical parameter to describe the capability of the potential trap, is $V_{\rm S} = V + V_0 - (V_0^2 + 2VV_0)^{1/2}$, where $V = V_{\rm PG} - V_{\rm FB} - Q_{\rm S}/C_{\rm OX}$, $V_0 = \varepsilon_s\varepsilon_0 qN_{\rm A}/C_{\rm OX}^2$ and $C_{\rm OX} = \varepsilon_{\rm OX}/T_{\rm OX}$. The boundary condition that the voltage $V_{\rm M}$ at the "drain" of the traditional photogate is enough to make the bipolar junction photogate operating at the saturated region is adopted. Therefore, the photocurrent $I_{\rm ph}$ and the output voltage V_{p2} can be written as

$$V_{p2} = \Big[-\sqrt{\beta}(V_{\rm S} + \alpha)I_0 + \alpha\sqrt{\beta}\ln I_{\rm ph} + I_0\sqrt{\beta(V_{\rm S} + \alpha)^2 + I_{\rm ph}}\Big]/(\sqrt{\beta}I_0), \tag{3}$$

where $V_{\rm M}$ is determined by $I_{\rm ph} = \beta V_{\rm M}[V_{\rm M} + 2(V_{\rm S} + \frac{kT}{q})]$, the gain factor $\beta = \frac{u_n C_{\rm OX} W}{2L}$ and the constant $\alpha = kT/q$. Compare Eq. (1) with Eq. (3), the following results can be obtained. Firstly, because the readout voltage of the new logarithmic pixel circuit is independent of the load transistor, the additive offset voltage from different pixels can be decreased and the quality of the image from a pixel array can be improved. Secondly, the output voltage swinging the new logarithmic pixel circuit have increased because the power supply is larger than the bias voltage of the load device and drops largely in the BJPG. The large output voltage benefits to increase the readout rate of the photo-charges. Thirdly, the load transistor in the new circuit can be manufactured in minor size, however, the load device of traditional logarithmic pixel circuit needs the large W/L ratio to obtain the required resistor.

At room temperature (T = 300 K), we considered a BJPG which is fabricated on a p-type substructure with the channel length L = 1 μm, the channel width W = 10 μm and the oxide thickness $T_{\rm OX}$ = 10 nm. The main physical parameters in the new device are: the grid voltage $V_{\rm PG}$ = 3.3 V, the intrinsic carrier density $n_i = 1.45 \times 10^{10}$ cm^{-3}, the impure density $N_a = 1 \times 10^{15}$ cm^{-3}, the doping concentration in the p^+ region $N_{p+d} = 1 \times 10^{16}$ cm^{-3}, the elementary charge $q = 1.602 \times 10^{-19}$ C, the generated photo-charge is 1×10^{-10} C, the electron mobility u_n = 1350 cm^2/V·s, and the dielectric constant of oxide $\varepsilon_{\rm OX} = 3.45 \times 10^{-13}$ F/cm. Figure 3 shows the simulation results for new logarithmic pixel circuit of the pixel voltage V_{p2} versus the photocurrent $I_{\rm ph}$. It is shown that the pixel output signal voltage is logarithmically related with the incident light power, which helps to enhance the dynamic range.

The BJPG is actually a compound device, which is equivalent to a photogate cascaded p^+n junction as shown in Fig. 1(b). The total noise of BJPG is the sum of that of the equivalent photogate and the equivalent diode. The former mainly includes the channel thermal noise, the signal charge transfer noise, the shot noise, the gate induced noise and $1/f$ noise; the latter mainly involves the shot noise and $1/f$ noise.

The gate-induced noise, a new type of noise proposed for BJPG, is brought about by the photoelectrons in the polysilicon gate of BJPG when the light is incident on the CMOS imager chip. When the light from the environment shows on the BJPG, the photoelectrons may be excited in the gate of BJPG, which will beget the gate voltage's fluctuation so as to result in the channel current's fluctuation via the gate capacitance and then bring about the gate-induced noise.

Assuming that the gate voltage varies with $\Delta V_{\rm G}$ and the induced charges ΔQ_n equals to the number of photoelectrons excited in the polysilicon gate of BJPG, the equation $\overline{\Delta Q_n^2} = C_{\rm gs}^2\overline{\Delta V_{\rm G}^2}$ can be obtained, where $C_{\rm gs} = C_{\rm OX}WL$ is the total gate-source capacitance. The noise current $\overline{i_{\rm d}^2}$ results from the fluctuation of the channel barrier distribution, which varies with the channel induced charges ΔQ_n because of the channel current's fluctuation and satisfies the formula $\overline{i_{\rm d}^2} = \overline{(j \cdot \omega \cdot \Delta Q_n)^2}$ (ω is the angle frequency). Therefore

$$\overline{i_{\rm d}^2} = \omega^2 C_{\rm gs}^2\overline{\Delta V_{\rm G}^2}. \tag{4}$$

On the other hand, the gate voltage fluctuation $\Delta V_{\rm G}$ results in the drain-source current's variation. If both $\Delta V_{\rm G}$ and $i_{\rm d}$ approximately meet the small signal current-

voltage relation,

$$\overline{i_d^2} = \overline{(g_m \cdot \Delta V_G)^2}. \tag{5}$$

$\overline{i_d^2}$ obeys the noise power density function $\overline{i_d^2} = S_I(f) \cdot \Delta f$, where Δf is the testing bandwidth, $S_I(f) = 4kT\gamma g$ is the average square value of the fluctuation i in the unit bandwidth around the frequency f, γ is an infinitude measurement factor that reflects the influence of the channel thermal noise due to the underlay deflection effect, and g is the transconductance. The BJPG cut-off frequency is $\omega_T = g/C_{gk}$, so

$$\overline{i_d^2} = 4 \cdot k \cdot T \cdot \gamma \cdot \Delta f \cdot g \cdot (\frac{\omega}{\omega_T})^2. \tag{6}$$

The power spectrum of the gate induced noise

$$S_g(f) = 4 \cdot k \cdot T \cdot \gamma \cdot g \cdot (\frac{\omega}{\omega_T})^2. \tag{7}$$

From Eq. (3), we can get

$$g = \frac{1}{R} = \frac{2I_0\sqrt{\beta(V_S + \alpha)^2 + I_{ph}}}{2\alpha\sqrt{\beta(V_S + \alpha)^2 + I_{ph}} + I_0^2 I_{ph}}. \tag{8}$$

The average square value $\sqrt{S_g(f)}$ is relative to the ratio of the angle frequency $\frac{\omega}{\omega_T}$ and the photocurrent I_{ph}, as shown in Fig. 4. From Fig. 4, the gate-induced noise does hardly change with the photocurrent, however, but becomes serious when the frequency of the noise voltage of the gate is near to the BJPG cut-off frequency.

The $1/f$ noise in the BJPG comes from both the photogate channel and the p^+n injecting junction. The main source of the channel $1/f$ noise in BJPG is the surface carriers fluctuation which results from the carriers shift ratio fluctuation induced by the oxidation trap charge fluctuation. The channel $1/f$ noise power spectrum is[10]

$$S_{\Delta I_D}(y, f) = (\frac{I_D}{W\Delta y})^2(\frac{R}{N} + \alpha u)^2 S_{\Delta N_t}(y, f), \tag{9}$$

where W is the channel width, u is the carriers transition ratio, N denotes the channel carriers density per unit area, and the power spectrum of the unit area trap charge fluctuation is $S_{\Delta N_t}(y, f) = \frac{kTW\Delta y}{\theta f} N_t(E_{Fn})$. In general, the coefficient R is 1. α is the scattering coefficient. Since the Fermi energy level changes along the channel direction y, $N_t(E_{Fn})$ also varies along the channel direction y and does not uniformly distribute with the energy level. If the $1/f$ noise power spectrum in the BJPG channel requires to be accurately calculated, the detailed formulas of $N(y)$, $a(y)$, $u(y)$ and $N_t(E_{Fn})$ must be known. However, their real value is relative to the adopted process. Therefore, one method is to adopt the semi-empirical relationship to simulate the channel $1/f$ noise characteristics.

The $1/f$ noise in the p^+n injecting junction comes of the compound velocity fluctuation of the junction surface. Under the assumption that the total current through the junction is constant and the p^+n junction $1/f$ noise takes place in the surface of the junction space charge region, the p^+n junction $1/f$ noise power spectrum is

$$S_I(f) = \frac{C_S}{f} I_S^2, \tag{10}$$

where the junction compound current is $I_S = qV_S p_1 \exp(qV_1/kT)A_S$. A_S is the valid compound area and C_S is the equivalent junction capacitance. The hole density at the voltage $V = 0$ and the surface compound velocity are expressed by p_1 and V_S, respectively. Therefore, the p^+n junction $1/f$ noise power spectrum is in direct proportion to the compound velocity. Figure 5 shows that the $1/f$ noise power spectrum $\sqrt{S_I}$ in the p^+n injection junction changes with the frequency f and the surface compound velocity V_S.

When the signal charge packages transfer along the BJPG channel, a fraction of signal charges will be left after every transfer cycle of the channel. The loss process of the signal charge is random, and therefore the signal charge package among many charge transfer cycles is the characteristics of the random fluctuation, resulting in signal charge transfer noise. In general, the transfer loss can be fallen into the signal charge transfer loss and the trap loss, the former is in direct proportion to the signal charge and the latter is relative with the interface state density. In general, for the BJPG operating in the low frequency, the interface state captured noise is the main of the signal charge transfer noise. The empty interface state can capture the signal electrons and the captured signal electrons are also set free. The capturing and launching processes are random and will bring about the carrier fluctuation. Under the condition that the interface state density N_{ss} is constant, the fluctuation of the captured electrons by the interface state results in the interface state captured noise. The induced signal

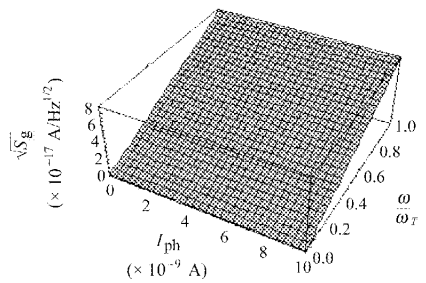

Fig. 4. The average square value $\sqrt{S_g}$ is relative to the $\frac{\omega}{\omega_T}$ and I_{ph}.

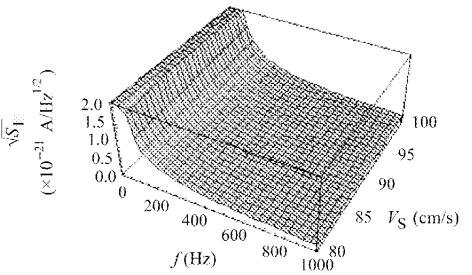

Fig. 5. $1/f$ noise power spectrum $\sqrt{S_I}$ in the p^+n injection junction changes with the frequency f and the surface compound velocity V_S.

electron fluctuation in the unit area interface state is[12]

$$\overline{\Delta N_{SS}^2} = 0.7kTN_{ss}. \quad (11)$$

Considering the two fluctuations of both capturing and launching processes, Eq. (11) should be multiplied by 2. Under the operating clock f_c, the power spectrum distribution of signal charge transfer noise is

$$S_{tr}(f) = 2.8(kT/q)Nf_cN_{ss}A_S(1 - \cos 2\pi f/f_c). \quad (12)$$

Figure 6 shows that the signal charge transfer noise power spectrum in the p^+n injection junction changes with the low frequency f.

To the BJPG, the thermal noise comes from the equivalent channel and the p^+n junction resistor which is relative with the illumination and bias conditions. The similar single-stage DC model of the BJPG is shown in Eq. (3). Therefore the power spectrum density of the BJPG thermal noise is

$$S_r(f) = \frac{8kT\gamma I_0\sqrt{\beta(V_S+\alpha)^2 + I_{ph}}}{2\alpha\sqrt{\beta(V_S+\alpha)^2 + I_{ph}} + I_0^2 I_{ph}}, \quad (13)$$

where γ is a coefficient, when the BJPG operates in the linear region, $\gamma \approx 1$, and in the saturation region, $\gamma \approx 2/3$. Figure 7 illustrates that the normalized thermal noise power spectrum decreases with the increasing photo-current.

With a p^+n injecting junction introduced into the BJPG device, there exists the shot noise. The probability of a certain signal charge going over the p^+n injection junction potential lies on whether the signal charge has enough energy and on the speed magnitude pointed at the junction surface. In the small injection condition, two parts of the junction current must be considered, one is the diffusion current from the p^+ region injecting to the n region, whose value is $I_0\exp(qV_d/kT)$; the other is the hole current $-I_0$ produced in the n region and collected by the p^+ region. Here I_0 denotes the inversion saturation current and V_d denotes the voltage drop of p^+n injecting junction. The power spectrum density of the p^+n injection junction shot noise is

$$S_I(f) = 2qI_0[\exp(qV/kT) + 1]. \quad (14)$$

Figure 8 shows that the shot noise power spectrum in p^+n injection junction region arises with the increasing junction voltage drop.

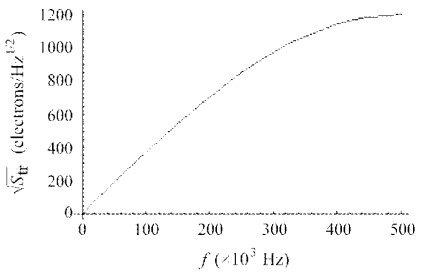

Fig. 6. Signal charge transfer noise power spectrum in the p^+n injection junction changes with the frequency f.

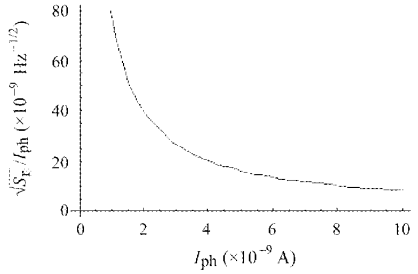

Fig. 7. The normalized thermal noise power spectrum to the photo-current decreases with the photo-current increasing.

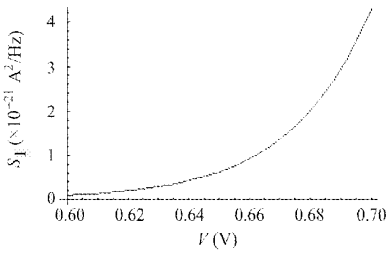

Fig. 8. Shot noise power spectrum in p^+n injecting junction region arises with increasing junction voltage drop.

In conclusion, a new and high performance device, BJPG, is proposed. Due to an introduced p^+n injecting junction, the BJPG can increase the readout rate of the pixel signal charges and improve the photoelectron transferring efficiency. Using this new device, a new type of logarithmic pixel circuit is obtained with a wide dynamic range. The noise characteristics of BJPG are analyzed in detail and a new gate-induced noise is proposed. Based on the established numerical analytical model of noise, the power spectrum density curves are simulated using the software Mathematica 4.0.

X. Jin's e-mail address is xiangliangjin@163.com.

References

1. E. R. Fossum, IEEE Trans. on Electron. Devices **44,** 1689 (1997).
2. D. X. D. Yang, A. E. Gamal, B. Fowler, and H. Tian, IEEE J. Solid-State Circuits **34,** 1821 (1999).
3. S. Decker, R. D. McGrath, K. Brehmer, and C. G. Sodini, IEEE J. Solid-State Circuits **33,** 2081 (1998).
4. S. Kavadias, B. Dierickx, D. Scheffer, A. Alaerts, D. Uwaerts, and J. Bogaerts, IEEE J. Solid-State Circuits **35,** 1146 (2000).
5. S. Collins, J. Ngole, and G. F. Marshall, Electron. Lett. **36,** 1806 (2000).
6. M. Schanz, W. Brockherde, R. Hauschild, B. J. Hosticka, and M. Schwarz, IEEE Trans. on Electron. Devices **44,** 1699 (1997).
7. J. Chang, A. Abidi, and C. Viswanathan, IEEE Trans. on Electron. Devices **41,** 1965 (1994).
8. H. Tian, B. Fowler, and A. E. Gamal, IEEE J. Solid-State Circuits **36,** 92 (2001).
9. H. S. Lee and L. G. Heller, IEEE Trans. on Electron. Devices **ED-19,** 1270 (1972).
10. K. K. Hung, K. K. Ping, C. M. Hu, and Y. C. Cheng, IEEE Trans. on Electron. Devices **ED-37,** 654 (1990).
11. D. F. Barbe, Electron. Lett. **8,** 207 (1972).
12. M. F. Tompsett, IEEE Trans. on Electron. Devices **ED-20,** 45 (1973).